Features of nuclear magnetic relaxation of water and benzene molecules during absorption on activated carbons and estimation of pore size distribution in adsorbents

E. V. Khozina,[a] R. Sh. Vartapetyan,[a] and D. Sh. Idiyatullin[b]*

[a]Institute of Physical Chemistry, Russian Academy of Sciences,
31 Leninsky prosp., 119991 Moscow, Russian Federation.
Fax: +7 (095) 952 5308. E-mail: vartapet@phyche.ac.ru
[b]Institute of Biochemistry and Biophysics, Kazan Research Center of the Russian Academy of Sciences,
Post Box 30, 420503 Kazan, Russian Federation

Nuclear magnetic relaxation in activated carbon—water and activated carbon—benzene adsorption systems was studied by pulse NMR methods. Activated carbons characterized by different porous structures and chemical state of the surface were used. The application of the three-pulse Goldman—Shen sequence to the adsorption system generates a dipole echo caused by the dipole-dipole coupling of "structural" protons, which is not averaged due to their mobility during experiment. The non-exponential character of relaxation attenuations of the transverse and longitudinal nuclear magnetizations of physically adsorbed molecules in activated carbon pores is a result of differencies in pore sizes. The pore sizes in activated carbon and the size distribution were determined from the data of nuclear magnetic relaxation with allowance for the contribution from the "structural" protons.

Key words: adsorption, activated carbons, nuclear magnetic relaxation, three-pulse Goldman—Shen sequence, dipole echo, pore size distribution.

Parameters of the porous structure of activated carbons (AC) are established,[1,2] as a rule, from analysis of experimental adsorption isotherms for nitrogen vapor at 77 K or benzene vapor at 293 K. The empirical dependence of the characteristic energy of adsorption can be used to derive the micropore size distribution from the experimental isotherms.[3,4] In recent years, based on the studies of the mechanism of water vapor adsorption on porous and nonporous AC, the methods for estimation of the micropore widths[5] and mesopore surface of AC [6] from H_2O adsorption were described. The analysis of comparison plots is used with this purpose: the adsorption isotherms of water vapor in the AC under study are compared with that observed on the surface of nonporous graphitized carbon black, where isolated water clusters are formed.[7]

An independent information on the state of adsorbed molecules and the porous structure of adsorbents, including AC, can be obtained by pulse NMR methods. Changes in the physical properties, in particular, mobility of adsorbed molecules, can be monitored using the study of changes in the nuclear magnetic relaxation (NM relaxation) parameters of adsorbate molecules. Moreover, the NMR method provides an information on the properties of the porous system, which induced these changes.

The theory of NM relaxation of molecules in pores is extensively described.[8—10] The nuclear magnetic relaxation of a molecule in the pore volume is determined by its interactions with surrounding similar molecules, and the corresponding relaxation time is t_b. Near the surface of pore walls or in the surface layer with the λ thickness, relaxation occurs on the so-called surface sinks of nuclear magnetization (surface functional groups, lattice defects, *etc.*) with the corresponding relaxation time t_s. Due to collisions with immovable or slow-moving particles, relaxation on the surface occurs much more rapidly than in the volume, *i.e.*, $t_s \ll t_b$ (conditions of NMR relaxation acceleration near the surface[11,12]).

If a substance introduced into a pore does not form chemical bonds with the pore surface, the thermal motion (self-diffusion) induces exchange between molecules in the surface layer and in the pore volume. Under conditions of rapid diffusion (when the relaxation time considerably exceeds the time needed for the molecule to cover distances comparable with the pore size), the relaxation

Published in Russian in *Izvestiya Akademii Nauk. Seriya Khimicheskaya,* No. 11, pp. 1881—1887, November, 2002.

1066-5285/02/5111-2036 $27.00

Table 1. Parameters of the AC porous structure[a] calculated from the adsorption isotherms of nitrogen vapor at 77 K (I) and water vapor at 293 K (II)

FAS	I							II, analysis of comparison plots[5]		
	BET equation		DR equation		DS equation					
	S_{BET}	S_{me}	W_0	x_0/nm	W_0	x_0	δ	S'_{me}	a_m	x_0/nm
	$m^2\ g^{-1}$		/$cm^3\ g^{-1}$		$cm^3\ g^{-1}$	nm		/$m^2\ g^{-1}$	/mmol g^{-1}	
1	680	30	0.32	0.24	0.32	0.24	0.06	28	0.24	0.25
2	1600	120	0.60	0.66	0.62	0.67	0.30	150	0.15	0.65
3	2300	340	—	—	—	—	—	360	0.13	0.90
	(2100)[b]									(0.8)[b]

[a] S_{BET} is the specific surface according to BET, S_{me} is the mesopore surface, W_0 is the micropore volume, x_0 is the half-width of micropores for the slit-like model, δ is the dispersion of the pore size distribution, and a_m is the number of primary adsorption sites for adsorption of water molecules.
[b] Determined by the comparison method.

time is proportional[11] to the characteristic pore size, *viz.*, the ratio of the pore size V to the surface S

$$t_i = V/\mu S \sim x,\ i = 1, 2, \qquad (1)$$

where $\mu = \lambda/t_s$ is the so-called surface magnetization strength.

This relation served as a basis for analysis of numerical measurements of the NM relaxation of liquids in different porous materials. In particular, the data on the NM relaxation of water[13] were used for the development of the algorithm for the estimation of the pore size distribution in model porous glasses, and the ratio of the transverse to longitudinal relaxation times of water in pores formed due to the random packing of glass balls was used to analyze the pore size distribution and connectivity.[14] The principal possibility to obtain an information on the parameters of the AC porous structure using relation (1) was shown.[15] The intervals of a possible change in the pore sizes were estimated by analysis of the data on the NM relaxation of adsorbed water and benzene. It is implicitly assumed in the calculations that the surface relaxation is uniform over the whole sample and the parameter of surface magnetization strength is excluded.

As a rule, activated carbon particles contain H atoms entering the composition of compounds chemically bound to the surface or belonging to the AC structure. These "structural" slow-moving protons can make a substantial contribution to the proton resonance signal and, hence, influence results obtained. Therefore, their contribution should be separated from the contribution of protons of adsorbed molecules. The special Goldman—Shen (GS) sequence with the pulse magnetic field gradient (PMFG) was used to study slow (in the NMR time scale) motions in complex polymeric systems.[16]

In this work we attempted to apply the refined method of estimation of the porous structure of microporous AC using pulse NMR to estimate the contribution from "structural" protons and to study the features governing mechanism of water and benzene adsorption in AC.

Experimental

Activated carbon samples with progressive degree of activation **1**, **2**, and **3** were prepared under laboratory conditions from furfural. Like their industrial analog (AC with the FAS trade mark produced by the Neorganika Joint-Stock Co. (Elektrostal, Moscow Region, Russia)), they are characterized by the virtually complete absence of ash admixtures.* Table 1 contains the data on the porous structure of these samples[15,17] calculated from the adsorption isotherms of nitrogen vapor at 77 K according to the Dubinin—Radushkevich (DR)[18] and Dubinin—Stoecki (DS)[19] equations and by the adsorption isotherms of water vapor.[5]

As can be seen from the data in Table 1, samples **1** and **2** with the micropore half-widths x_0 = 0.24 and 0.66—0.67 nm, respectively, refer to the typical microporous AC. Sample **2** is characterized by larger micropores, a broader size distribution of micropores (parameter δ), and a larger mesopore surface. Sample **3** with a pore half-width of 0.8 nm belongs to supermicroporous AC according to Dubinin´s classification. The Brunauer—Emmett—Teller (BET) equation and the comparison method for estimation of the micropore parameters were used for the determination of the porous structure parameters of sample **3**.[20]

The adsorption isotherms of water and benzene vapors on samples **1** and **2** at 293 K are presented in Fig. 1. The difference between the adsorption isotherms for benzene and water is due to the fact that the dispersion interaction plays the main role in benzene adsorption, whereas the adsorption of water results in the formation of hydrogen bonds between H_2O and oxygen-containing acidic surface groups, *viz.*, primary adsorption sites (PAS). Benzene is predominantly adsorbed in micropores, in

* The authors thank V. V. Gur´yanov for kindly presented samples.

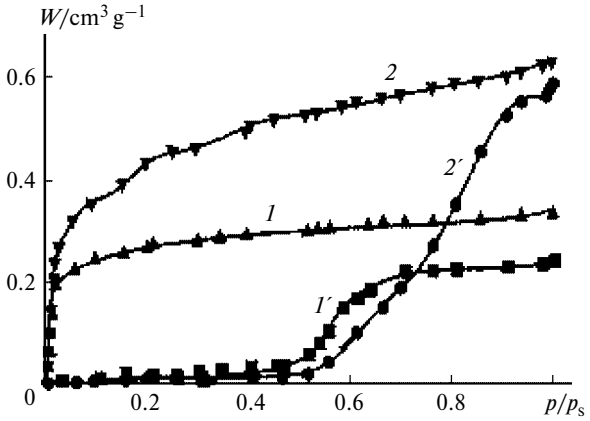

Fig. 1. Adsorption isotherms of benzene (*1*, *2*) and water (*1′*, *2′*) vapors on samples **1** (*1*, *1′*) and **2** (*2*, *2′*) at $T = 293$ K.

which the adsorption energy is higher. As the degree of adsorption is progressively increased, wider and wider pores are filled,[2,3,18] whereas water is adsorbed[5] first on PAS, which can be in both micropores and wider pores. In the low-pressure region, the water adsorption is proportional[5] to the surface concentration of PAS. Adsorbed water molecules play a role of secondary adsorption sites on which clusters of H_2O can be formed by hydrogen bonds. The adsorption isotherms of water vapor on sample **2** are described by flatter curves than those of sample **1**, indicating a broader pore distribution in sample **2**. The "tail" at $p/p_s > 0.95$ for sample **2** indicates a significant adsorption of water on the mesopore surface.[6]

The AC samples were filled with the adsorbate as follows. An AC weighted sample was evacuated in a thin-walled tube at 673 K for 2 h and weighted. The sample was evacuated again, and a specified amount of the substance was injected using a microsyringe through the vacuum compression into an ampule, which was preliminarily placed in a Dewar flask with liquid nitrogen. Then the ampule was sealed off, and the amount of the adsorbed substance was monitored by repeated weighting. The coverage (θ) was determined with respect to the micropore volume found by analysis of the adsorption isotherms. Samples completely saturated with water (with all pores filled) were prepared by pouring of a weighted sample with water and removal of a water excess by evaporation. The sealed ampule was stored at 373 K for several hours to equalize the adsorbate concentration in AC granules. After cooling, the ampule was placed in the cell of an NMR spectrometer, whose temperature was maintained constant.

NMR experiments were carried out on the apparatus developed at the Chair of Molecular Physics of the Kazan State University[7,15] (proton resonance 19 MHz, magnetic field gradient 0.1 T m^{-1}, interval of measured relaxation times $1 \cdot 10^{-5}$—5 s). Transverse relaxation processes were examined by free induction decay (FID) signals, which followed the sequences of radio-frequency pulses $90°_x$—τ—$90°_y$—τ—"solid-echo."[21] The modified GS sequence with PMFG[16] was used to isolate the contribution from "structural" protons. The PMFG amplitude with a duration of 10 μs was 0.1 T m^{-1}. The time of recovery of the magnetic field uniformity did not exceed 10 μs. The Carr—Purcell—Meiboom—Gill (CPMG) sequence[22,23] was used to determine the transverse relaxation time (t_2). The longitudinal relaxation time (t_1) was measured using the sequence of radio-frequency (RF) pulses $(90°_x—\tau_1—90°_y—\tau_1—90°_x—\tau_2—180°—\tau_2)_n$,[24] which allows the measurement of the magnetization attenuation during "one passage." In this case, pulses with the durations $\tau_1 = 10$ μs and $\tau_2 = 10$ ms were used. Nuclear magnetization decays were approximated by the sum of exponential functions, where the number of addends did not exceed three. The correlation coefficient in approximation was 97—98%. The t_1 and t_2 values were determined with an accuracy of at least 10%. Measurements were carried out at 303 K.

Results and Discussion

Modified Goldman—Shen experiment. The contributions from "structural" protons of activated carbon and protons of physically adsorbed water and benzene molecules need to be separated to obtain reliable data on the porous structure of activated carbons using the NM relaxation parameters. With this purpose we used the GS sequence with PMFG ($90°_x—\tau_1—90°_{-x}—\delta—\tau_2—90°_x—t$), which has previously been proposed for studying slow motions in complex polymeric systems.[16]

The results of quantum-mechanical calculations of the response from the system consisting of two isolated spins to the sequence of three radio-frequency pulses were described for the case when the spin-spin interactions are not averaged due to the mobility during characteristic intervals and the dipole-dipole interactions are predominant.[21] The following expression was obtained for the magnetization of the system $M(t)$ that is generated by the application of the GS sequence (response of the system):

$$M(t) = 0.5\left\langle \cos\frac{\psi(\tau_1) - \psi(t)}{2} + \cos\frac{\psi(\tau_1) + \psi(t)}{2} \right\rangle, \qquad (2)$$

where $\psi(\tau_n)$ is the change in the phase of spins induced by the dipole-dipole interactions during the interval τ_n, and <...> means the averaging over all states of the spin system. The first term describes the appearance of the dipole echo at the moment $t = \tau_1$, which is imposed on the decrease in the transverse magnetization determined by the second term.

The results indicating the appearance of the dipole echo were confirmed by the experimental data for the samples of polymeric networks and, in part, crystalline polyethylene glycols.[21]

The response of the system of spins to the GS sequence, $M(t)$, can be expressed through the function of FID $g(t)$[25]:

$$M(t) = 0.5g(\tau_1)g(t)(x + 1/x), \qquad (3)$$

where $x = g(\tau_1 + \tau_2)g(\tau_2 + t)/[g(\tau_2)g(\tau_1 + \tau_2 + t)]$.

Then the independent measurement of $g(t)$ and the response of the system of spins to the application of the GS sequence ($M(t)$ function) makes it possible to check different models of mobility in the system of spins. In fact, in the system of stationary protons the FID is described by the Gauss function

$$g(t) = \exp(-t^2W_2/2), \quad (4)$$

where W_2 is the second momentum of the NMR absorption line.

Then the response to the GS sequence is the so-called dipole echo, being the result of dipole coupling, which was not averaged due to the mobility of protons

$$M(t) = 0.5\{\exp[-(\tau_1 + t)^2W_2/2] + \exp[-(\tau_1 - t)^2W_2/2]\}, \quad (5)$$

where τ_1 is the interval between the first and second 90-degree RF pulses in the three-pulse GS sequence. The first term corresponds to the continuation of the FID from the moment $\tau_1 + t$, and the second term is a function with the maximum in the point $t = \tau_1$, *i.e.*, dipole echo. In the case of the fast isotropic movement, the response of the system to the application of the pulse sequence coincides with the exponential FID function with the corresponding relaxation time t_2.

Figure 2 exemplifies the FID signals and responses of the system to the GS sequence with PMFG obtained at different τ_1 values and the unchanged value of $\tau_2 \to 0$ (the least possible value, in our case, $\tau_2 = 30$ μs) for the C_6H_6—**3** sample with the coverage $\theta = 0.09$ at $T = 303$ K. The FID function (the curve corresponding to $\tau_1 = 0$ in Fig. 2) is described as the sum of two components

$$g(t) = pf_f(t) + (1 - p)f_s(t), \quad (6)$$

where f_f is the fast relaxation function, whose fraction in the total signal is $p = 0.7$, and f_s is the slow relaxation function. In this case, f_s is approximated by an exponential function and corresponds to the relaxation of benzene molecules in pores of sample **3**. The rapidly relaxing component is difficult to approximate by this or another function.

The response of the system to the pulse GS sequence also includes the sum of two functions (the curves for $\tau_1 =$ 10—80 μs in Fig. 2)

$$M(t) = pM_f(t) + (1 - p)M_s(t), \quad (7)$$

where $M_f(t)$ and $M_s(t)$ are the functions of the rapidly and slowly decreasing magnetizations, respectively.

The appearance of the dipole echo in the $M(t)$ curves for $\tau_1 = 10$—80 μs (see Fig. 2) at the moment τ_1 directly points to the presence of slow-moving protons, whose relaxation is described by the Gauss function. It is the Gauss function that can describe the free induction signal, which was observed in the study of the AC sample evacuated at 673 K. The FID function for sample **1** is presented as an example in Fig. 3. It is seen that in the

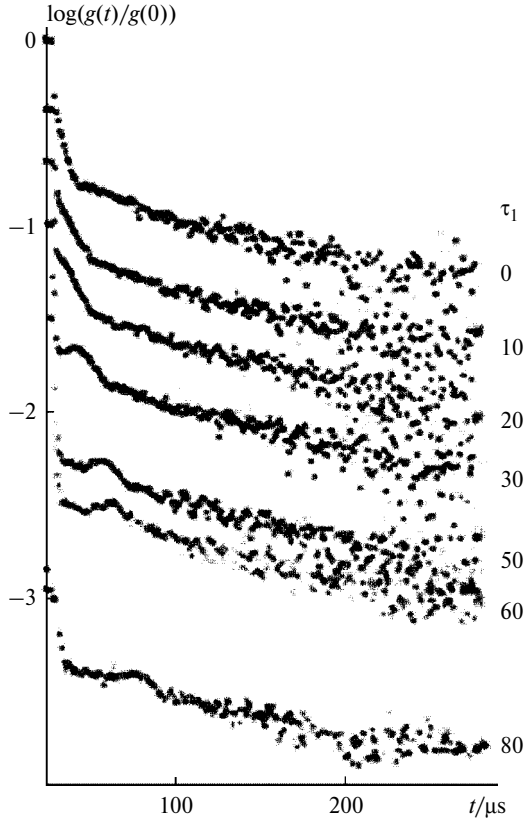

Fig. 2. Free induction decay following the single 90-degree RF pulse ($\tau_1 = 0$) and responses to the application of the GS sequence with PMFG ($\tau_1 = 10$—80 μs, the τ_1 values are presented in the figure) for the **3**—C_6H_6 sample at $\theta = 0.09$ ($\tau_2 = 30$ μs).

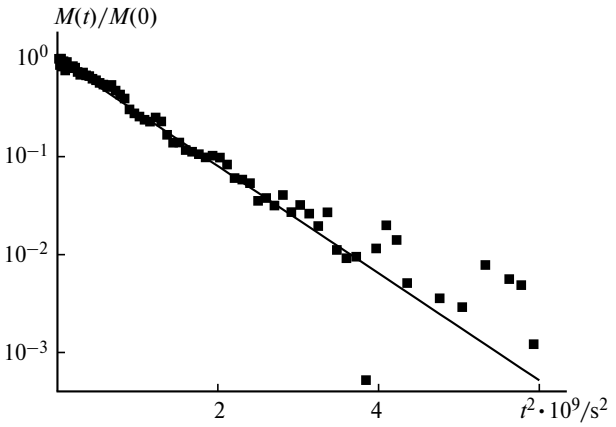

Fig. 3. Free induction decay in sample **1** after its evacuation at 673 K. The straight line corresponds to the approximation of the FID by the Gauss function with the second momentum equal to $0.93 \cdot 10^{10}$ G^2.

$\log[M(t)/M(0)]$—t^2 coordinates the plot of a change in the FID function represents a straight line, *i.e.*, it is described by the Gauss function (4).

The facts described above indicate that the rapidly relaxing FID component in the benzene (water)—AC systems is determined by the contribution from slow-moving "structural" protons, whose relaxation is caused by the dipole-dipole coupling. The attenuation of the echo with an increase in the τ_1 parameter (see Fig. 2) indicates the partial averaging of the dipole-dipole interactions due to mobility of protons. This implies that the introduction of an adsorbate into AC pores affects the mobility of the "structural" H atoms. It is probably the non-inertness of the adsorbent, which is thus manifested during adsorption. Examples for the adsorption deformation of adsorbents, in particular, AC, are available in the literature.[26]

Determination of parameters of the AC porous structure from longitudinal and transverse relaxation. The attenuation function of the transverse magnetization $M(t)$ in the C_6H_6—**2** system at $\theta = 0.6$ is shown in Fig. 4. The function was obtained at $\tau = 100$ μs using the CPMG sequence, which excludes the contribution from structural protons. The function describes the relaxation of physically adsorbed benzene molecules and, as can be seen in the figure, represents the sum of two exponents with the corresponding relaxation times t_2^{min} and t_2^{max}.

The conditions of "rapid" diffusion are fulfilled in the systems studied, because the time needed for water or benzene molecules with a self-diffusion coefficient of $\sim 1 \cdot 10^{-9}$ $m^2\ s^{-1}$ to traverse pores with the size x = 1—100 nm is $1 \cdot 10^{-10}$—$1 \cdot 10^{-11}$ s, which is much less than the minimum relaxation time t_2^{min}. In this case, each pore is characterized by its relaxation time, and the observed distribution of t_2 corresponds to the distribution of molecules over pores of this or another size[11]

$$P(t_{2i}) \rightarrow P(x_i). \quad (8)$$

In addition, the multicomponent character of the attenuation function of nuclear magnetization indicates that the adsorbent bulk contains fragments with predominantly large and small pores, *i.e.*, with different porosities.

By analogy to the previous procedure,[15] the following proportion based on Eq. (1) can be written for each AC sample with a specified coverage by benzene or water:

$$t_2^{max}/x_{max} = t_2^{min}/x_{min}. \quad (9)$$

This allows the estimation of sizes of the corresponding pores. Note that the influence of the surface relaxivity (surface magnetization strength) is excluded in this case. The strength of surface magnetization is assumed to remain unchanged with an increase in the coverage of the sample.

Thus, using the expansion of the attenuation function of transverse magnetization to the components t_2^{min} and t_2^{max}, one can estimate the maximum sizes of carbon pores (x_{max}) containing adsorbed water or benzene molecules. The minimum pore size is considered equal to the dimensions of adsorptives, *i.e.*, 0.30 nm for water (width) and 0.37 nm for benzene (thickness). The validity of this assumption is corroborated by the fact that transverse relaxation times of ~1 ms are observed during adsorption of water molecules in ultramicroporous activated carbon, whose pores are inaccessible for larger molecules.[27]

The x_{max} values calculated using relation (9) with allowance for the size of the benzene molecule are presented in Table 2 for three benzene—FAS systems. The broadest pore size distribution is observed in the C_6H_6—**2** system. This conclusion agrees with the data obtained by the study of nitrogen and water adsorption (see Table 1). The averaged t_2 values, which were determined from the formula $1/t_2^{av} = \sum_i p_i/t_{2i}$, are 1.3, 8.4, and 9.5 ms for the C_6H_6—**1**, C_6H_6—**2**, and C_6H_6—**3** systems, respectively,

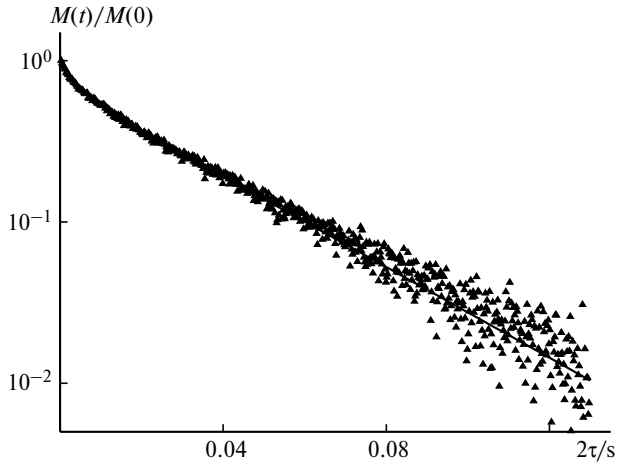

Fig. 4. Decay in the transverse magnetization in the C_6H_6—**2** sample at $\theta = 0.6$ due to the application of the CPMG sequence (the interval between the π-pulses is 100 μs). The solid line is the approximation of attenuations by the sum of two exponential functions with the relaxation times t_2^{min} and t_2^{max}.

Table 2. Expansion of attenuations of $M(t)/M(0)$ of benzene in FAS samples **1**, **2**, and **3** to the components t_2^{min} and t_2^{max} and the calculated by Eq. (9) maximum size of FAS **1**—**3** pores (x_{max}) in which benzene is adsorbed at $\theta = 0.6$

Sample FAS	t_2^{min}	t_2^{max}	x_{max}/nm
	ms		
1	0.8	2.9	1.4
2	3.5	31	3.2
3	7.6	46	2.2

which is in accord with the sequence of changing in the mean size of micropores $2x_0$ in the same systems (see Table 1). (Note that the procedure of determination of micropore sizes from adsorption data give similar results for nitrogen and benzene adsorption, because the parameters of the DR equation for these adsorbates are related through the affinity coefficient.)[18]

Thus, there is a possibility to find the distribution of molecules over pores of this or another size in the adsorption system considered. The data obtained from the transverse relaxation times t_2 agree with the results for longitudinal relaxation (t_1). The attenuation function of longitudinal magnetization is also polyexponential, and the condition of fast diffusion is fulfilled. The estimations of the pore size distribution from the data of longitudinal and transverse relaxation give close results (Fig. 5), which follows from the theory[8,9] (see Eq. (1)).

For the C_6H_6—**3** sample, the widths of micropores with the maximum "weight" (fraction of pores of a specific size) found from t_1 (1.43 nm) and t_2 (1.60 nm) do not differ from the mean pore size $2x_0$ = 1.8 nm calculated from water adsorption (see Fig. 5, Table 1). However, the maximum pore widths in sample **1**, which were estimated using the same t_1 and t_2 parameters (2.11 and 1.77 nm, respectively), exceed remarkably the mean micropore size calculated from the adsorption data: $2x_0 = 0.48 \pm 0.12$ nm. A similar discrepancy was observed for the porous structure of activated carbon **1** studied by X-ray small-angle scattering.[28] Note, however, that the pore width calculated from t_1 and t_2 of benzene correspond to the characteristic scale of micro- ($x \leq 2$ nm) and mesopores ($2 < x \leq 50$ nm) at a sufficiently great coverage of the adsorbent.

The maximum size of pores (x_{max}), in which water is adsorbed, estimated from relation (9) under the condition that $x_{min} \approx 0.3$ nm, *i.e.*, equal to the size of the water

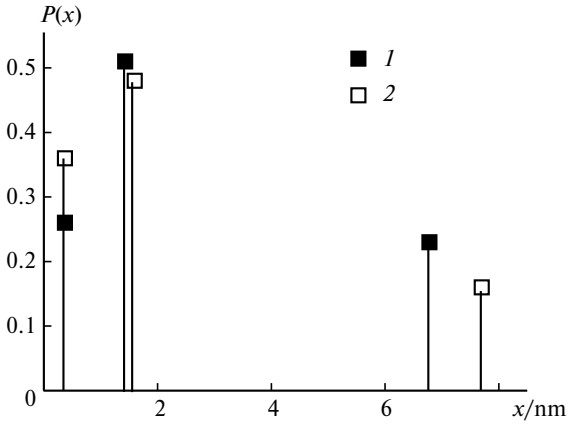

Fig. 5. Distribution of benzene molecules over pores with specific sizes in the C_6H_6—**3** system at the complete micropore filling according to the data of measurements of t_1 (*1*) and t_2 (*2*) for benzene.

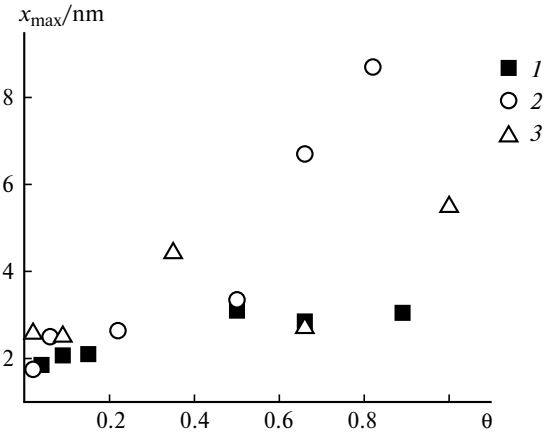

Fig. 6. Plots of the maximum size of the filled pores in samples **1** (*1*), **2** (*2*), and **3** (*3*) for water adsorption *vs.* coverage of the adsorbent.

molecule,[1] increases in the series of FAS samples **1** < **3** < **2**. For the water-saturated samples, the interval of the relaxation time distribution for water in pores of sample **2** (10—135 ms) is the broadest, while for samples **1** and **3** it is 6.9—61 and 13—90 ms, respectively. This indicates a broader pore size distribution in sample **2**.

The plots of x_{max} *vs.* θ for three different water—FAS systems presented in Fig. 6 allow the comparison of the water distribution in pores of the AC under study, and they reflect the pore size distributions in these adsorbents. The x_{max} value increases with an increase in θ in sample **3** and especially sample **2**, which also indicates a wider pore distribution in the latter case.

According to the adsorption data, benzene is predominantly adsorbed in micropores, while the water adsorption is determined by the presence of PAS on the pore walls. Let us compare the distributions of water and benzene molecules over pores of samples **1**, **2**, and **3** at different coverages (Fig. 7). The data were obtained by the NM relaxation method (measurement of t_2). Note that the distribution of adsorbate molecules characterized by the relaxation times t_{1i} and t_{2i} over pores with the size x_i is related, in any case, to the pore size distribution in AC and the PAS concentration (for the water adsorption).

Analysis of the NMR data on the benzene and water distributions in pores of samples **1**, **2**, and **3** allows the following conclusions to be made.

1. Sample **1** is characterized by the maximum fraction of micropores ($x \leq 2.1$ nm) in the total pore volume, and the micropore widths found by measurements of the NM relaxation are greater than the values obtained using the adsorption isotherms of nitrogen and water. The micropore widths do not exceed 2.75—3.1 nm.

2. Sample **2** is characterized by the broadest pore size distribution among three activated carbons studied, and

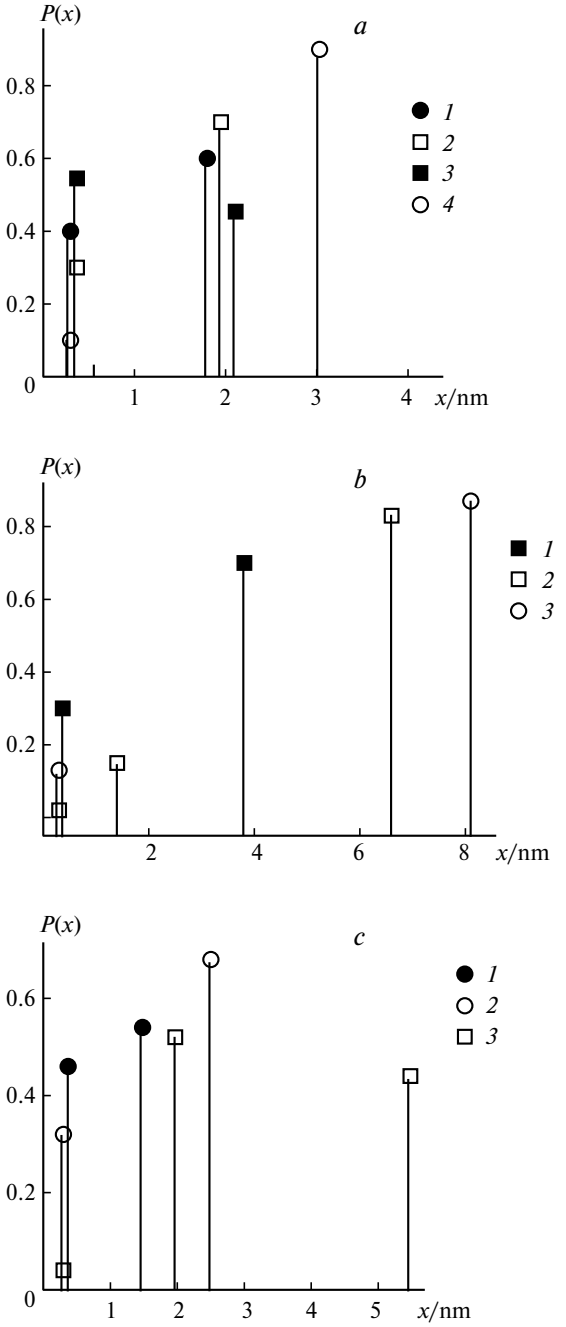

Fig. 7. Distribution of water and benzene over pores in samples of activated carbons **1** (*a*), **2** (*b*), and **3** (*c*): *a*. θ = 0.05, benzene (*1*), water (*2*); θ = 1, benzene (*3*); θ = 0.89, and water (*4*); *b*. θ = 0.6, benzene (*1*), water (*2*), and sample completely saturated with water (*3*); *c*. θ = 0.1, benzene (*1*), water (*2*); θ = 1, and water (*3*).

mesopores prevail in the total pore volume. The limiting size of mesopores is ≥8.1 nm, and the fraction of water molecules adsorbed in mesopores of sample **2** is higher than that for **3** due to a sufficiently great number of PAS in mesopores of **2**.

3. In sample **3** the pore size distribution is also reasonably broad, and the number of mesopores in this sample is greater than that in sample **1**. However, the PAS concentration in mesopores of sample **1** is lower than that for sample **2**.

Thus, with the use of the modified pulse GS sequence of the dipole echo in the benzene—AC adsorption system was experimentally detected. Due to this, one can separate the contributions to the attenuation of the transverse magnetization from protons chemically bound to the AC surface and from physically adsorbed benzene and water molecules. A reliable information on the porous structure of adsorbents can be obtained by the analysis of the distribution of relaxation times of benzene and water in pores of the AC studied taking into account the contribution from "structural protons." The obtained estimates agree with the concepts on the mechanisms of benzene and water adsorption on activated carbons. According to these concepts, benzene is predominantly adsorbed in micropores and then, with an increase in the amount adsorbed, in mesopores. Adsorbed water is distributed in both micro- and mesopores, depending on the distribution and concentration of primary adsorption sites.

This work was financially supported by the Russian Foundation for Basic Research (Project No. 00-03-32060).

References

1. S. J. Gregg and K. S. W. Sing, *Adsorption, Surface Area and Porosity,* Academic Press, New York, 1982.
2. M. M. Dubinin, *Izv. Akad. Nauk SSSR, Ser. Khim.*, 1991, 9 [*Bull. Acad. Sci. USSR, Div. Chem. Sci.*, 1991, **40**, 1 (Engl. Transl.)].
3. M. M. Dubinin, *Carbon*, 1983, **21**, 359.
4. H. F. Stoeckli, P. Rebstein, and L. Ballerini, *Carbon*, 1990, **28**, 907.
5. R. Sh. Vartapetyan and A. M. Voloshchuk, *Usp. Khim.*, 1995, **64**, 1055 [*Russ. Chem. Rev.*, 1995, **64**, 985 (Engl. Transl.)].
6. R. Sh. Vartapetyan, A. M. Voloshchuk, G. A. Petukhova, and N. S. Polyakov, *Izv. Akad. Nauk, Ser. Khim.*, 1993, 2048 [*Russ. Chem. Bull.*, 1993, **42**, 1960 (Engl. Transl.)].
7. R. Sh. Vartapetyan, R. B. Klarkson, B. M. Odintsov, A. V. Filippov, and V. D. Skirda, *Kolloid. Zh.*, 2000, **62**, 590 [*Colloid J.*, 2000, **62**, 526 (Engl. Transl.)].
8. K. R. Brownstein and C. E. Tarr, *J. Magn. Reson.*, 1977, **26**, 17.
9. K. R. Brownstein and C. E. Tarr, *Phys. Rev., A.*, 1979, **19**, 2446.
10. R. L. Kleinberg, W. E. Kenyon, and P. P. Mitra, *J. Magn Reson. Ser., A.*, 1994, **108**, 206.
11. H. Cohen and K. S. Mendelson, *J. Appl. Phys.*, 1982, **53**, 1127.
12. J. Korringa, D. O. Seevers, and H. C. Torrey, *Phys. Rev.*, 1962, **127**, 1143.

13. F. D´Orazio, J. C. Tarcson, and W. Halperin, *J. Appl. Phys*., 1989, **65**, 742.
14. B. P. Hills and J. E. Snaar, *Mol. Phys.*, 1995, **84**, 141.
15. R. Sh. Vartapetyan, A. M. Voloshchuk, E. V. Khozina, I. Yu. Aslanyan, A. I. Maklakov, and V. D. Skirda, *Kolloid. Zh*., 1999, **61**, 764 [*Colloid J*., 1999, **61**, 707 (Engl. Transl.)].
16. D. Sh. Idiuatullin, V. D. Skirda, and E. V. Khozina, *J. Magn. Reson. Ser. A*, 1995, **117**, 137.
17. E. V. Khozina, R. Sh. Vartapetyan, and A. M. Voloshchuk, *Kolloid. Zh*., 1997, **59**, 252 [*Colloid J*., 1997, **59** (Engl. Transl.)].
18. M. M. Dubinin and L. V. Radushkevich, *Dokl. Akad. Nauk SSSR*, 1947, **55**, 331 [*Dokl. Phys. Chem.*, 1947 (Engl. Transl.)].
19. M. M. Dubinin and H. F. Stoeckli, *J. Coll. Int. Sci.*, 1980, **75**, 34.
20. R. Sh. Michail, S. Brunauer, and E. E. Bodor, *J. Colloid. Int. Sci.*, 1968, **26**, 45.
21. M. H. Levitt and R. Freeman, *J. Magn. Reson*., 1981, **43**, 65.
22. H. Y. Carr and E. M. Purcell, *Phys. Rev.*, 1954, **94**, 630.
23. S. Meiboom and D. Gill, *Rev. Sci. Instr.*, 1958, **29**, 6881.
24. D. Sh. Idiyatullin, V. D. Skirda, and V. S. Smirnov, Author´s Certificate 1578608 (USSR), *Byul. Izobret*. [*Invention Bulletin*], 1990, 9854 (in Russian).
25. D. Sh. Idijatullin, V. D. Skirda, and E. V. Khozina, *Extended Abstr. of the XXVII Congress AMPERE*, Kazan, August 21—28 1994, **2**, 605.
26. A. A. Fomkin, N. I. Regent, and V. A. Sinitsyn, *Izv. Akad. Nauk, Ser. Khim*., 2000, 1018 [*Russ. Chem. Bull., Int. Ed.*, 2000, **49**, 1012].
27. R. Sh. Vartapetyan, A. M. Voloshchuk, M. M. Dubinin, I. Kerger, and G. Pfaifer, *Izv. Akad. Nauk SSSR, Ser. Khim.*, 1985, 2425 [*Bull. Acad. Sci. USSR, Div. Chem. Sci.*, 1985, **34**, 2241 (Engl. Transl.)].
28. G. M. Plavnik and T. P. Puryaeva, *Kolloid. Zh.*, 2000, **62**, 524 [*Colloid J.*, 2000, **62** (Engl. Transl.)].

Received April 20, 2001;
in revised form March 5, 2002